

# Continual Adversarial Defense

Qian Wang<sup>1</sup> Yaoyao Liu<sup>2</sup> Hefei Ling<sup>1,\*</sup> Yingwei Li<sup>2</sup> Qihao Liu<sup>2</sup> Ping Li<sup>1</sup>  
 Jiazhong Chen<sup>1</sup> Alan Yuille<sup>2</sup> Ning Yu<sup>3,\*</sup>

<sup>1</sup>Huazhong University of Science and Technology <sup>2</sup>Johns Hopkins University <sup>3</sup>Salesforce Research  
 {yqwq1996, lhefei, lpshome, jzchen}@hust.edu.cn  
 {yliu538, yingwei.li, qliu45, ayuille1}@jhu.edu ning.yu@salesforce.com

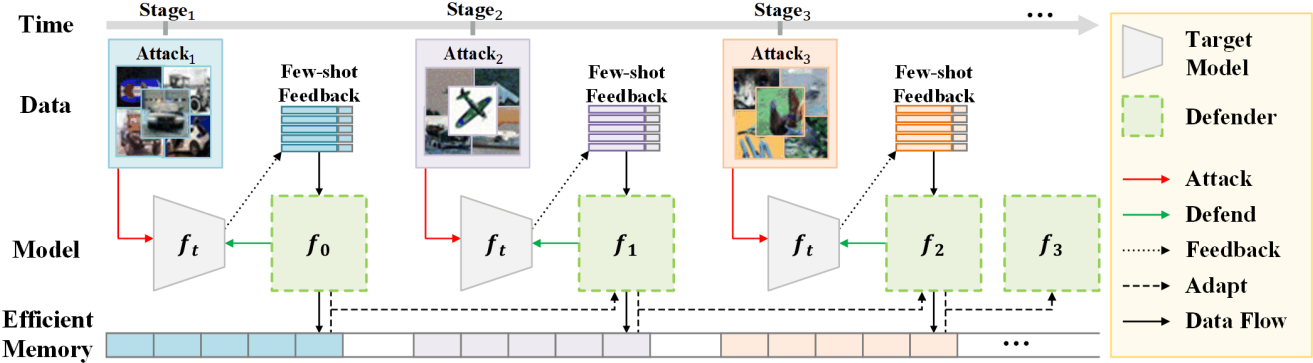


Figure 1. In a dynamic environment, the target model  $f_t$  faces a diverse range of attacks at different stages and is protected by the defender. During the  $i$ -th stage, the defender  $f_i$  leverages few-shot defense feedback provided by the security department and users of the target model to adapt to new attacks. The defender also needs to efficiently use memory to store the cache, retaining knowledge of past attacks.

## Abstract

In response to the rapidly evolving nature of adversarial attacks on a monthly basis, numerous defenses have been proposed to generalize against as many known attacks as possible. However, designing a defense method that can generalize to all types of attacks, including unseen ones, is not realistic because the environment in which defense systems operate is dynamic and comprises various unique attacks used by many attackers. The defense system needs to upgrade itself by utilizing few-shot defense feedback and efficient memory. Therefore, we propose the first continual adversarial defense (CAD) framework that adapts to any attacks in a dynamic scenario, where various attacks emerge stage by stage. In practice, CAD is modeled under four principles: (1) continual adaptation to new attacks without catastrophic forgetting, (2) few-shot adaptation, (3) memory-efficient adaptation, and (4) high accuracy on both clean and adversarial images. We leverage cutting-edge continual learning, few-shot learning, and en-

semble learning techniques to qualify the principles. Experiments conducted on CIFAR-10 and ImageNet-100 validate the effectiveness of our approach against multiple stages of 10 modern adversarial attacks and significant improvements over 10 baseline methods. In particular, CAD is capable of quickly adapting with minimal feedback and a low cost of defense failure, while maintaining good performance against old attacks. Our research sheds light on a brand-new paradigm for continual defense adaptation against dynamic and evolving attacks.<sup>1</sup>

## 1. Introduction

In recent years, deep neural networks have been widely used in numerous vision tasks [30], leading to remarkable breakthroughs. However, many neural networks are vulnerable to adversarial attacks, which aim to deceive a classifier by adding subtle perturbations to input images, thus altering prediction results. This vulnerability seriously jeopardizes the reliability of deep neural networks, particularly in

\*Corresponding authors

<sup>1</sup>Code at <https://github.com/cc13qq/CAD>

security- and trust-sensitive domains.

Researchers have proposed various general defense methods against adversarial attacks. As a standard defense method, adversarial training [44] aims to enhance the robustness of the target model by training it with adversarial examples. Another branch of adversarial defense involves purifying the data stream [41] to remove potential adversarial perturbations or noise that could deceive the model. However, models of adversarial training often exhibit reduced classification accuracy on adversarial examples and may sacrifice classification capacity on clean images. On the other hand, purification techniques may appear more reliable, but the denoising procedure can inadvertently smooth the high-frequency texture of clean images, potentially causing issues for the target model.

From an application perspective, it is not realistic to design a defense method that can generalize to all types of attacks, including unseen ones. The truth is, the increasing number of defense strategies naturally stimulates the development of new attack algorithms [32]. As a result, the defense system encounters a dynamic environment characterized by numerous unique attacks with higher success rates in both white-box and black-box settings [16]. The target model is threatened by many attackers with various attacks, just like the defense scenario against Deepfake [10].

To simulate a dynamic environment more realistically, we propose a defense scenario that considers practicality. As illustrated in Fig. 1, the attacker employs diverse attacks at different stages to target the model, while the defender adapts to emerging attacks by leveraging few-shot defense feedback. In this paper, we use adversarial examples with ground truths as the defense feedback, which is provided by the security department and users of the target model in real-world situations. In this ongoing “arms race,” the attacker operates within the gray-box setting [32], where they possess knowledge of the classifier’s architecture and have access to training data but are unaware of the defense mechanism in place. On the other hand, the defender has the same training data and access to the target model, but also possesses full knowledge of the initial attack.

Taking real-world considerations into account, we propose four principles for the scenario: (1) *Continual adaptation to new attacks without catastrophic forgetting*. As defenders, it’s essential to adapt to various new attacks at different stages while retaining knowledge of previous ones. (2) *Few-shot adaptation*. Increased feedback indicates more successful attacks on the target model. Therefore, we cannot afford too many successful attacks before upgrading the defense. (3) *Memory-efficient adaptation*. Over time, a continuous influx of attacks results in accumulating defense feedback, potentially leading to memory constraints. In practical terms, we may not have sufficient memory capacity to withstand this. (4) *High accuracy in classifying*

*both clean and adversarial images*. A robust defense should not compromise the interests of those it protects. Hence, maintaining high classification accuracy on both clean and adversarial images is crucial.

In this paper, we propose the Continual Adversarial Defense (CAD) framework, which aims to defend against evolving attacks in a stage-by-stage manner using few-shot defense feedback and efficient memory. In the first stage, we train an initial defense model using adversarial images from the initial attack. This model is specifically designed to classify images with adversarial noise, complementing the target model. Drawing inspiration from continual learning (CL), we expand the classification layer to adapt to the new attack as incremental classes. We then fine-tune this expanded layer using few-shot defense feedback. To address the over-fitting issue that arises from the few-shot fine-tuning process, we reserve embedding space in the defense model for future attacks. This is achieved by generating and assigning virtual prototypes, which help compress the embedding of previous attacks. To optimize memory usage in the data domain, we employ prototype augmentation which allows us to maintain the decision boundary of previous stages without the need to store any feedback explicitly. Simultaneously, we utilize a small model to ensemble the defense model with the target model by estimating reliable logits for input images, ensuring maximum classification accuracy for both clean and adversarial images.

Based on our comprehensive experiments conducted on CIFAR-10 and ImageNet-100, the CAD framework demonstrates strong performance in defending against multi-stage attacks relying on few-shot feedback while maintaining high accuracy on clean images. Our main contributions can be summarized as follows:

- In order to simulate the rapidly evolving adversarial attacks against image classifiers, we introduce, for the first time, a dynamic scenario of various attacks that emerge in different stages. The defender is required to adapt to new attacks using few-shot defense feedback and efficient memory, while also retaining knowledge of previous attacks and upholding high performance on both clean and adversarial images.
- We propose the Continual Adversarial Defense (CAD) framework that defends against attacks in the dynamic scenario under four practical principles: continual adaptation without catastrophic forgetting, few-shot adaptation, memory-efficient adaptation, and high accuracy in classifying both clean and adversarial images. We leverage cutting-edge techniques including continual learning, few-shot learning, non-exemplar class incremental learning, and ensemble learning to satisfy the principles.

- Extensive experiments on CIFAR-10 and ImageNet-100 validate the effectiveness of CAD against multiple stages of 10 modern adversarial attacks using few-shot feed-

back and efficient memory, and demonstrate significant improvements over 10 baseline methods.

## 2. Related Work

### 2.1. Adversarial Attacks

Adversarial attacks [6] attempt to fool a classifier into changing prediction results by attaching subtle perturbations to the input images while maintaining imperceptibility from human eyes. PGD [26] and BIM [14] generate adversarial examples through several iterations of perturbation and get significantly improved attack performance. DIM [40], TIM [4], and SIM [17] improve the transferability under the black-box setting and breach several defense techniques. Incorporating variance tuning, VIM [38] achieves a high attack rate against multiple advanced defense methods. In this paper, a wide spectrum of attacks is used to offense the target model at different stages under the gray-box setting.

### 2.2. Adversarial Defense

Adversarial training [26, 45] is the mainstream of adversarial defense that uses attacked samples to train a robust model. TRADES [44] characterize the trade-off between accuracy and robustness for classification problems via decomposing the robust error as the sum of the natural error and the boundary error. JEM [7] uses energy-based training of the joint distribution and improves the calibration and robustness of target models. Replacing the denoising diffusion probabilistic model with the elucidating diffusion model, DMAT [39] improves adversarial training and achieves new SOTA robust accuracy.

Another technical solution for protecting DNNs from adversarial attacks is adversarial purification [9, 29], which aims to purify the data stream before feeding it into the target model, functioning under the gray-box setting [32]. Based on an EBM trained with Denoising Score-Matching, Yoon et al. [41] propose Adaptive Denoising Purification (ADP) which conducts purification in a randomized purification scheme. Nie et al. [27] propose DiffPure that uses the forward and reverse processes of diffusion models to purify adversarial images.

Certainly, both adversarial training and purification methods have shown limitations in robustness, leading to reduced classification performance on clean images. Furthermore, the dynamic nature of the environment introduces a diverse array of unique attacks employed by multiple attackers. In this paper, we propose Continual Adversarial Defense (CAD) framework as a solution to effectively combat various attacks emerging stage by stage, while maintaining strong performance in classifying clean images.

### 2.3. Continual Learning

Continual learning (CL) [18–25, 28, 46] aims to learn from a sequence of new classes without forgetting old ones and attracts much attention to various computer vision tasks. Many works have been proposed for CL: by introducing different knowledge distillation (KD) losses to consolidate previous knowledge [28], by preserving a small number of old class data (exemplars) or augmented data (Zhu et al., 2021) to recall the old class knowledge [49], and by expanding the network capacity for new class data or freezing partial network parameters to keep the old class knowledge [48]. In recent years, some methods have aimed to solve the CL problem without depending on preserving data (called none-exemplar) [51], and some methods have attempted to learn new classes in a few-shot scenario [43] in which only a small number of new class data is gainable. In this paper, we convert the proposed defense scenario into a few-shot and non-exemplar CL setting, which necessitates the defense mechanism to utilize few-shot defense feedback and efficient memory for adaptation.

## 3. Threat Model and Defense Principles

The defense system operates within a dynamic environment characterized by a multitude of unique attacks since the growing number of defenses naturally encourages the invention of new attack algorithms. Once frustrated by an existing defense, attackers undoubtedly resort to deploying various attacks in pursuit of breakthroughs. In response to this reality, we simulate the dynamic environment and put forth a practical threat model. In this threat model, attackers deploy different attacks in various stages to assault the target model, and the defender must adapt to evolving attacks by utilizing the defense feedback, just like an "arms race". The defense feedback is typically provided by security services and users of the target model upon the discovery of successful attacks during screening or cleanup efforts in the real world, and plays a critical role in informing and shaping the defender's response to emerging threats. In this paper, we use adversarial examples with ground truths as the defense feedback. We formulate this attack vs defense scenario as follows.

Our scenario is established on the  $N$ -way  $K$ -shot classification paradigm. The attacker attacks under the gray-box setting [32] in which the attacker knows the architecture of the target model  $f_t : \mathcal{X} \rightarrow \mathbb{R}^N$  which trained on  $\mathcal{D}_{\text{train}}$  and evaluated on  $\mathcal{D}_{\text{test}}$ , but blind to the defense, where  $\mathcal{X}$  is the image space. The defender is permitted to visit  $\mathcal{D}_{\text{train}}$  and has the full knowledge of the initial attack  $A_0(\cdot)$  at the 0-th stage. At the  $i$ -th stage, where  $i = 1, 2, \dots, T$ , the attacker knows the failure of previous attacks and turns to a new attack  $A_i(\cdot)$ . Meanwhile, the defender receives a set of feedback  $\mathcal{A}_{\text{train}}^i = \{(\mathbf{x}_{\text{adv}}^i, y) | \mathbf{x}_{\text{adv}}^i = A_i(\mathbf{x}), (\mathbf{x}, y) \in \mathcal{D}_{\text{train}}\}$

containing  $N \times K$  samples (i.e.,  $K$  samples for each of  $N$  classes) and uses it to adapt to the new attack. Evaluations are conducted on  $\mathcal{D}_{\text{test}}$  and  $\{\mathcal{A}_{\text{test}}^k\}_{k=0,1,\dots,i}$  at each stage  $i$ , where  $\mathcal{A}_{\text{test}}^i = \{(\mathbf{x}_{\text{adv}}^i, y) | \mathbf{x}_{\text{adv}}^i = A_i(\mathbf{x}), (\mathbf{x}, y) \in \mathcal{D}_{\text{test}}\}$ .

Taking reality into account, the defense mechanism should satisfy the following principles:

**Principle 1** *Continual adaptation to new attacks without catastrophic forgetting.*

In the dynamic environment, it is not uncommon for certain attackers to employ the same attack across different stages. Therefore, the defense mechanism must be capable of adapting to a range of new attacks in each stage while also retaining knowledge of previous ones.

**Principle 2** *Few-shot adaptation.*

The increase in defense feedback directly correlates with the frequency of successful attacks on the target model. As defenders, we must proactively adapt the defense based on few-shot feedback to prevent potential security disasters that could arise from delayed action following an abundance of feedback.

**Principle 3** *Memory-efficient adaptation.*

Over time, the ongoing influx of attacks results in accumulating defense feedback, potentially leading to the memory constraints. In practical terms, the defender may not have sufficient memory space to accommodate this accumulation. Consequently, storing all received defense feedback for adaptation is impractical and should be avoided.

**Principle 4** *High accuracy in classifying both clean and adversarial images.*

The previous defense strategies have led to a sacrifice in the classification accuracy of clean images, resulting in performance degradation. This decline could potentially have a negative impact on crucial real-world business operations. As a result, it is imperative for a defender to prioritize maintaining performance on both clean and adversarial images.

## 4. Continual Adversarial Defense Framework

As shown in Fig. 2, Continual Adversarial Defense (CAD) consists of continual adaptation to defend the target model while preventing catastrophic forgetting ( Sec. 4.1), embedding reservation to alleviate overfitting brought by the few-shot feedback ( Sec. 4.2), prototype augmentation for memory efficiency ( Sec. 4.3), and model ensemble to ensure the classification performance on both clean and adversarial images(Section 4.4).

### 4.1. Continual Adaptation to New Attacks

In response to Principle 1, we use continual adaptation to defend against new attacks while preventing catastrophic forgetting. In the 0-th stage, an initial defense model  $f_0 : \mathcal{X} \rightarrow \mathbb{R}^N$  which consists of a feature extractor  $\varphi : \mathcal{X} \rightarrow \mathbb{R}^d$  and a classifier  $g_c^0 : \mathbb{R}^d \rightarrow \mathbb{R}^N$  is optimized under the full supervision using adversarial dataset  $\mathcal{A}_{\text{train}}^0 = \{(\mathbf{x}_{\text{adv}}^0, y) | \mathbf{x}_{\text{adv}}^0 = A_0(\mathbf{x}), (\mathbf{x}, y) \in \mathcal{D}_{\text{train}}\}$ . The defense model is designed to tackle adversarial examples, complementing the target model. In the  $i$ -th stage, the defense model  $f_i : \mathcal{X} \rightarrow \mathbb{R}^N$  adapts to new attack using defense feedback  $\mathcal{A}_{\text{train}}^i$ . Inspired by continual-learning (CL) [28], we regard classes with the new attack as incremental classes and endow the defense model with scalability by classifier expansion.

Following [21], we expand the classifier from  $g_c^0 : \mathbb{R}^d \rightarrow \mathbb{R}^N$  to  $g_c^1 : \mathbb{R}^d \rightarrow \mathbb{R}^{N \times 2}$  in the first stage, and expand the classifier  $g_c^i$  from  $\mathbb{R}^d \rightarrow \mathbb{R}^{N \times i}$  to  $\mathbb{R}^d \rightarrow \mathbb{R}^{N \times (i+1)}$  at the  $i$ -th stage. The parameter of the expanded classifier is composed of the parameter of the old classifier and the newly initialized parameter:  $W^i = [W^{i-1}, W^{\text{new}}]$ , where  $W^i = [\mathbf{w}_1^i, \dots, \mathbf{w}_{N_i}^i]$  is the parameter matrix of  $g_c^i$  and  $N_i = N \times (i+1)$  is number of classes in stage  $i$  after expansion. Meanwhile, the ground truth of  $\mathcal{A}_{\text{train}}^i$  is rewritten corresponding to the incremental classes with the new attack <sup>2</sup>:

$$y^i = y + N \times i. \quad (1)$$

The initial defense model  $f_0$  will be trained in Sec. 4.2. After this, we freeze the feature extractor  $\varphi$  and fine-tune the part of the classifier expanded for the new attack  $A_i$  using few-shot feedback  $\mathcal{A}_{\text{train}}^i$  in Sec. 4.3.

For evaluation, we are just focusing on which class the image is placed in rather than being threatened by which attack. Thus the prediction for an instance  $\mathbf{x}$  is:

$$y_{\text{pred}} = (\arg \max f_i(\mathbf{x})) \% N \quad (2)$$

### 4.2. Embedding Reservation for Few-Shot Adaptation

A problem brought by the few-shot feedback in Principle 2 is over-fitting which is common in few-shot learning [31]. To tackle this issue, we choose to reserve embedding space for future attacks by generating and assigning virtual prototypes, squeezing the embedding space of previous attacks.

First, before training the defense model  $f_0$  at the 0-th stage, several virtual prototypes  $P_v = [\mathbf{p}_v^1, \dots, \mathbf{p}_v^V] \in \mathbb{R}^{d \times V}$  are pre-assign in the classifier and treated as ‘virtual classes’ [43], where  $V = N \times T$  is the number of virtual classes, i.e. the reserved classes for future attacks. Therefore the output of current model is  $f_0(\mathbf{x}) = [W^0, P_v]^{\top} \varphi(\mathbf{x})$ .

<sup>2</sup>We omit the networks’ parameter in formulas

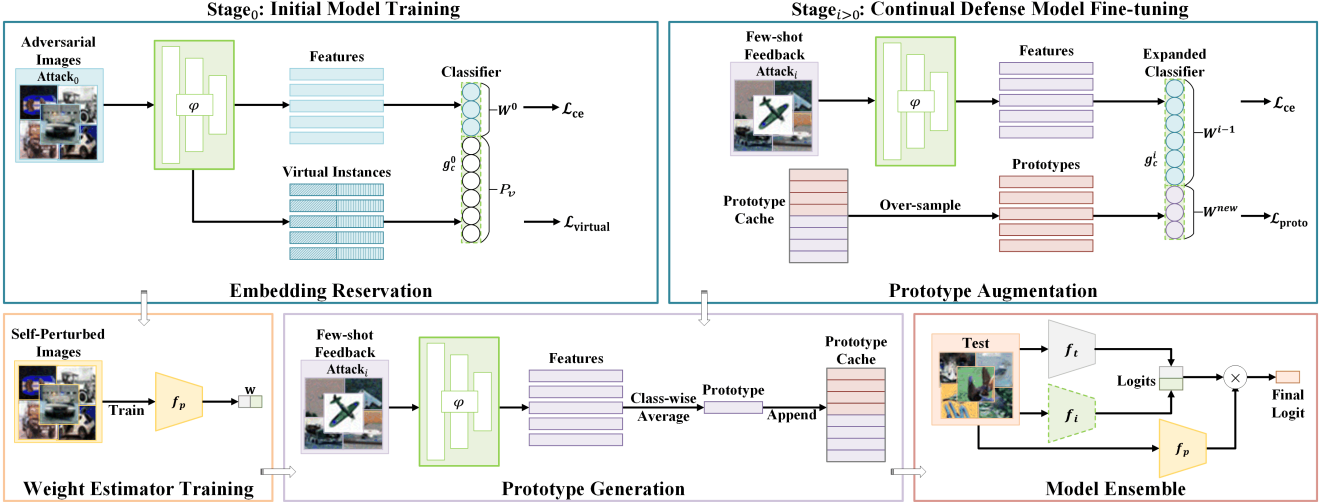


Figure 2. Illustration of CAD. Regarding the classes with new attacks as incremental classes, we use continual adaptation to protect the target model while preventing catastrophic forgetting. In the 0-th stage, we reserve the embedding space for future attacks during training of the initial defense model  $f_0$  to alleviate overfitting brought by future fine-tuning. And then, a weight estimator model  $f_p$  is trained for the model ensemble. In the  $i$ -th stage ( $i > 0$ ), we freeze the feature extractor  $\varphi$  of defense model  $f_i$  and fine-tune the expanded classifier  $g_c^i$  using few-shot defense feedback. To efficiently use memory, we store class-wise prototypes in the prototype cache at each stage and use them in the fine-tuning process. After all, the target model  $f_t$  and the scalable defense model  $f_i$  are ensembled by the weight estimator to maintain high accuracy of both clean and adversarial images.

Second, virtual instances are constructed by manifold mixup [36]:

$$\mathbf{z} = h_2(\lambda h_1(\mathbf{x}_{\text{adv},r}^0) + (1 - \lambda)h_1(\mathbf{x}_{\text{adv},s}^0)), \quad (3)$$

where  $\mathbf{x}_{\text{adv},r}$  and  $\mathbf{x}_{\text{adv},s}$  belong to different classes  $r$  and  $s$ , and  $\lambda \sim \text{B}(\alpha, \beta)$  is a trade-off parameter the same as [48].  $h_1$  and  $h_2$  are decoupled hidden layers of feature extractor i.e.  $\varphi(\mathbf{x}) = h_2 \circ h_1(\mathbf{x})$ .

Third, the embedding space reserving is conducted by training  $f_0$  with the following loss:

$$\mathcal{L}_v = F_{\text{ce}}(\text{Mask}(f_0(\mathbf{x}_{\text{adv}}^0), y^0), \hat{y}) + F_{\text{ce}}(f_0(\mathbf{z}), \hat{y}) + F_{\text{ce}}(\text{Mask}(f_0(\mathbf{z}), \hat{y}), \hat{y}). \quad (4)$$

where  $\hat{y} = \text{argmax}_j \mathbf{p}_v^{j\top} \varphi(\mathbf{x}_{\text{adv}}^0) + N$  is the virtual class with maximum logit, acting as the pseudo label.  $\hat{y} = \text{argmax}_k \mathbf{w}_k^{0\top} \mathbf{z}$  is the pseudo label among current known classes.  $\gamma$  is a trade-off parameter,  $F_{\text{ce}}$  represents the standard cross-entropy loss [47], and function  $\text{Mask}(\cdot)$  masks out the logit corresponding to the ground-truth:

$$\text{Mask}(f_0(\mathbf{x}_{\text{adv}}^0), y^0) = f_0(\mathbf{x}_{\text{adv}}^0) \otimes (\mathbf{1} - \text{onehot}(y^0)) \quad (5)$$

where  $\otimes$  is Hadamard product and  $\mathbf{1}$  is an all-ones vector. The final loss for training the initial defense model is:

$$\mathcal{L}_{\text{ce}} = F_{\text{ce}}(f_0(\mathbf{x}_{\text{adv}}^0), y^0), \quad \mathcal{L}_0 = \mathcal{L}_{\text{ce}} + \gamma \mathcal{L}_{\text{virtual}} \quad (6)$$

In Eq. (4), it forces an instance to be away from the reserved virtual classes (item 1) and pushes the mixed instance towards a virtual class (item 2) and away from other

classes (item 3). Trained with  $\mathcal{L}_0$ , the embedding of initial benign classes will be more compact, and the embedding spaces for virtual classes will be reserved [48]. The reserved space allows the defense model to be adapted more easily in the future and alleviates overfitting brought by few-shot feedback.

### 4.3. Prototype Augmentation for Memory Efficiency

In response to Principle 3, we use prototype augmentation to efficiently use memory.

When learning new classes, the decision boundary for previous classes can be dramatically changed, and the unified classifier is severely biased [50]. Many CIL methods store a fraction of old data to jointly train the model with current data to address this issue [28]. However, preserving old feedback may also lead to memory shortage. For memory efficiency, we adopt prototype augmentation [51] to maintain the decision boundary of previous stages, without saving any feedback. We memorize one prototype in the deep feature space for each class with each attack, and over-sample (i.e.,  $U_B$ ) prototypes  $\mathbf{p}_B$  and ground-truths  $y_B$  to the batch size, achieving the calibration of the classifier:

$$\mathbf{p}_B = U_B(P_e), \mathcal{L}_{\text{proto}} = F_{\text{ce}}(\mathbf{p}_B, y_B) \quad (7)$$

where  $P_e = \{\mathbf{p}_e^j\}_{j=0}^{N \times i}$  is the set of class-wise average embedding (i.e., prototype cache) generated by feature extrac-

tor  $f_e^i$  the same as ProtoNet [31]:

$$\mathbf{p}_e^j = \frac{1}{K} \sum_{k=1}^K \mathbb{I}(y_k^i = j) \varphi(\mathbf{x}_{\text{adv},k}^i) \quad (8)$$

where  $\mathbb{I}(\cdot)$  is the indicator function, and  $K$  is the amount of feedback for each class.

In each stage, the defense model is adapted using the following loss:

$$\mathcal{L}_{\text{ce}} = F_{\text{ce}}(f_i(\mathbf{x}_{\text{adv}}^i), y^i), \quad \mathcal{L}_f = \mathcal{L}_{\text{ce}} + \mathcal{L}_{\text{proto}} \quad (9)$$

---

#### Algorithm 1 Continual Adversarial Defense

---

**Input:** Benign dataset  $\mathcal{D}_{\text{train}}$ , initial attack  $A_0$ , target model  $f_t$ , and few-shot feedback  $\mathcal{A}_{\text{train},K}^i$  generated by attack  $A_i$  for stage  $i = 1, \dots, T$ .

**Output:** Defense model ensemble.

- 1: Generate initial adversarial dataset  $\mathcal{A}_{\text{train}}^0$  using  $A_0$ .
- 2: Train weight estimator  $f_p$  on  $\mathcal{D}_{\text{train}}$  using self-perturbation.
- 3: Rewrite the ground-truth of  $\mathcal{A}_{\text{train}}^i$  using Eq. (1).
- 4: Optimize defense model  $f_0$  on  $\mathcal{A}_{\text{train}}^0$  using Eq. (5).
- 5: Generate prototypes of  $A_0$  using Eq. (8) and add them to prototype set  $P_e$ .
- 6: **for**  $i$  in  $1, \dots, T$  **do**
- 7:   Fine-tune the part of the classifier preserved for the new attack using Eq. (9).
- 8:   Generate prototypes of  $A_i$  using Eq. (8) and add them to prototype set  $P_e$ .
- 9:   Ensemble the defense model  $f_i$  and the target model  $f_t$  using Eq. (10).
- 10: **end for**

---

#### 4.4. Model Ensemble for Clean and Adversarial Image Classification

To maintain high classification accuracy on both clean and adversarial images mentioned in Principle 4, we propose the model ensemble as the last part of CAD. Ensemble adversarial training (EAT) [34] which trains a robust model using adversarial samples generated by the target model is a simple yet effective way to defend against adversarial attack under the gray-box setting while maintaining the classification performance of clean images. We extend EAT to our scenario by training a small weight estimator model  $f_p$  to fuse the logits of models

We adopt the self-perturbation [37] to train the weight estimator at the first stage. Agnostic to any of the attacks, a self-perturbation-trained model is able to distinguish images from benign and adversarial. Details of the self-perturbation are given in the supplementary.

The weight estimator  $f_p$  outputs a weight vector  $\mathbf{w} \in \mathbb{R}^2$  to ensemble the defense model and the target model:

$$\text{logit}_i(\mathbf{x}) = \mathbf{w} \cdot [f_t(\mathbf{x}), f_i(\mathbf{x})]^\top \quad (10)$$

In this way, both the clean images and the adversarial images are correctly classified.

The overall algorithm of CAD framework is presented in Algorithm 1.

## 5. Experiment

To validate the performance of CAD against various adversarial attack methods in the dynamic scenario, we conduct extensive empirical studies on two datasets and compare CAD to baselines from two research streams. For evaluation and analysis, we use two metrics in this section: (1) classification accuracy against each attack after adaptation. (2) the average of the accuracy of all attacks that have occurred in and before in each stage, i.e. average incremental accuracy [28].

**Datasets** CIFAR-10 [13] is a widely used dataset for adversarial attack and defense, containing 5000 images for training and 1000 images for testing in each of the 10 classes. ImageNet-100 [33] is a subset of ImageNet [1] and contains 100 classes with 1000 images for training and 100 images for testing in each class. Images from CIFAR-10 and ImageNet-100 are resized to  $32 \times 32$  and  $224 \times 224$  respectively. Before training, the above datasets endured data augmentation including horizontal flip and random crop.

**Attack algorithms** We select 11 adversarial attack methods PGD [26], FGSM [6], BIM [14], RFGSM [35], MIM [3], DIM [40], NIM [17], SNIM [17], VNIM [38], and VMIM [38] to compose the attack pool. The perturbation magnitude of all the attacks is set to  $\epsilon = 8$  under  $l_\infty$  following [44].

**Implementation details** Both the target model and defense model use ResNet as the backbone network in our method. Specifically, we use WideResNet-28-10 [42] for CIFAR-10 following [7] and ResNet-50 [8] for ImageNet-100 following [15]. A 4-layer ConvNet is used as the weight estimator model. The cosine classifier [5] is adopted as the classifier of the defense model. We utilize Torchattacks [12] for generating adversarial images. The amount of feedback per class is set to  $K = 10$ . The number of stages is set to  $T = 9$  since there are 10 attacks (PGD is the initial attack). Parameters of Beta distribution are set to  $\alpha = \beta = 2$  and the trade-off parameter for  $\mathcal{L}_0$  is set to  $\gamma = 0.01$  following [48]. Epochs for training  $f_0$  are set to 100 and fine-tuning epochs are set to 4.

**Baselines** We first compare to adversarial training methods TRADES [44], JEM [7], GAIRAT [45], FastAdv [11], RPF [2] and DMAT [39]. Besides, we propose another variant of our method denoted as premium-CAD in the case of no constraint of memory and no concerns about the amount of feedback. In premium-CAD, we train additional attack-specific defense models using abundant feedback (i.e., 1000 images per class) in each stage, and ensemble them with the target model by the weight estimator. Details about premium-CAD are given in the supplementary.

## 5.1. Comparisons to Baselines

We compared CAD to other baseline methods in defending against 10 adversarial attacks. In our approach, the defense environment is dynamic, with attacks occurring at different stages. In contrast, the other baseline methods operate in a static defense environment that does not differentiate the order of attacks. We report the robust accuracy, which measures the performance on adversarial examples generated by attacks, and the standard accuracy, which measures the performance on clean data, separately for each method. We compare the defense performance of our method to other methods on CIFAR-10 and ImageNet-100. All the evaluation is conducted on the whole test set.

As depicted in Tab. 1 and Tab. 2, despite the modest scale of feedback, both CAD and premium-CAD demonstrate strong adaptability to each type of attack. When compared with the top baseline methods DMAT [39] and ADP [41], CAD outperforms them by approximately 10% in CIFAR-10 and 6% in ImageNet-100 for each attack. This underscores its capacity for continuous adaptation in response to emerging attacks. Another notable advantage of CAD is its ability to maintain high classification performance for clean images, achieving 95.8% accuracy for CIFAR-10 and 88.1% for ImageNet-100, while the testing accuracy of the target model stands at 96.4% for CIFAR-10 and 89.8% for ImageNet-100. This can be attributed to the generic representation learned by the weight estimator for adversarial examples, enabling it to effectively differentiate between clean and adversarial images. We observe that the accuracy against FGSM is relatively lower than that for other attacks, largely due to the distinct noise pattern of the one-step FGSM compared to other attacks.

To assess CAD’s performance in mitigating catastrophic forgetting, we present the average incremental accuracy in Fig. 3. The curve initially experiences a slight decline in the first three stages before stabilizing. This temporary dip is primarily attributable to FGSM’s influence, which pulls down the entire curve, and the adaptation to new attacks, resulting in a minor decrease in accuracy against previous attacks. Subsequently, the curve exhibits a modest increase due to the resemblance of other attacks to the initial attack PGD, thereby elevating the overall curve. Throughout the

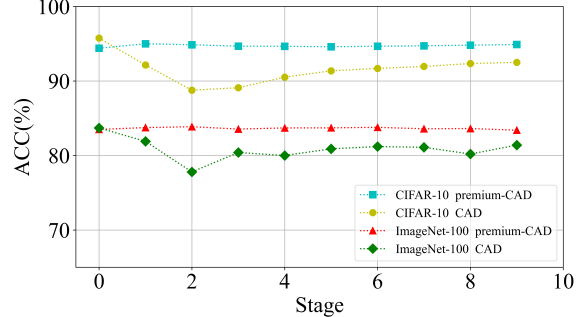


Figure 3. Average incremental accuracy (%) of CAD.

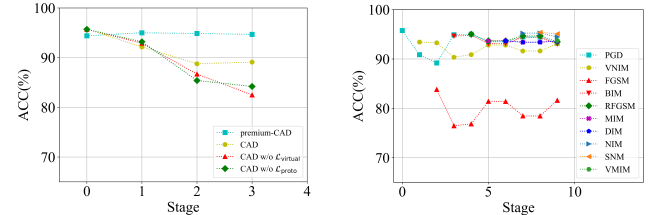


Figure 4. Accuracy (%) in each stage on CIFAR-10. Left: average incremental accuracy of ablation. Right: classification accuracy against each attack.

evaluation, the curves consistently hover around 92% for CIFAR-10 and 80% for ImageNet-100, underscoring CAD’s robust capacity to counter catastrophic forgetting.

Note that premium-CAD outperforms all baseline methods. Given adequate defense feedback and memory resources, premium-CAD emerges as the superior choice.

## 5.2. Ablation Study

As argued, embedding reservation allows the defense model to be adapted more easily in the future and alleviates overfitting, prototype augmentation maintains the decision boundary of previous stages, and model ensemble ensures robust classification performance for both clean and adversarial images. Subsequently, we proceed to undertake an ablation study to validate the efficacy of each component.

As shown in Tab. 3 and Fig. 4 (Left), CAD without  $L_{\text{virtual}}$  and  $L_{\text{proto}}$  experiences a decrease of 13.2% and 2.2% respectively in performance for adaptation. Furthermore, the absence of model ensemble results in the defense model’s inability to uphold classification accuracy for clean images alone. Additionally, we present curves illustrating the classification accuracy of each attack in Fig. 4 (Right). These curves demonstrate that the adaptation of CAD to FGSM is comparatively less effective than for other attacks, aligning with our earlier observations about FGSM in Sec. 5.1.

## 5.3. Multiple Attacks in One Stage

In practice, it is common for multiple attacks to occur simultaneously within a single stage. To assess CAD’s adapt-

Stage Attack	0 PGD	1 VNIM	2 FGSM	3 BIM	4 RFGSM	5 MIM	6 DIM	7 NIM	8 SNIM	9 VMIM	- Clean
TRADES [44]	55.8	57.4	60.7	55.9	55.8	57.1	57.1	58.9	60.2	57.3	84.8
JEM [7]	55.8	46.5	60.7	52.3	52.4	51.1	51.4	57.0	62.0	48.2	91.7
PAT [15]	45.5	43.8	49.8	45.5	45.3	45.2	45.2	43.9	45.1	45.4	69.3
GAIRAT [45]	66.9	66.4	68.3	66.9	66.7	66.5	66.5	68.6	70.4	66.4	89.4
FastAdv [11]	37.1	36.8	41.9	37.0	37.7	37.7	54.6	36.4	39.6	37.6	75.2
RPF [2]	60.9	52.2	58.0	58.9	54.9	57.6	57.5	53.5	52.8	52.6	83.5
DMAT [39]	71.7	73.1	75.8	71.7	71.7	73.0	73.0	75.5	76.0	73.0	92.4
EBM [9]	75.2	73.0	70.0	76.6	76.5	72.4	73.9	74.0	72.9	73.8	86.8
ADP [41]	85.4	79.3	82.0	84.4	85.1	84.1	83.7	81.0	80.5	79.1	80.5
DiffPure [27]	72.5	69.8	71.8	70.1	72.2	73.4	73.5	72.7	70.2	69.4	89.3
<b>CAD(ours)</b>	<b>95.8</b>	<b>93.4</b>	<b>83.8</b>	<b>94.7</b>	<b>95.0</b>	<b>93.7</b>	<b>93.7</b>	<b>95.2</b>	<b>95.4</b>	<b>93.7</b>	<b>95.8</b>
<b>CAD<sup>†</sup>(ours)</b>	<b>94.4</b>	<b>95.6</b>	<b>94.6</b>	<b>94.1</b>	<b>94.6</b>	<b>94.3</b>	<b>95.1</b>	<b>95.1</b>	<b>95.5</b>	<b>95.7</b>	<b>96.0</b>

Table 1. Classification accuracy (%) against various attacks on CIFAR-10. Column "Clean" represents the standard accuracy of clean images. **CAD<sup>†</sup>** denotes premium-CAD that is not constrained by the efficient memory and few-shot defense feedback.

Stage Attack	0 PGD	1 VNIM	2 FGSM	3 BIM	4 RFGSM	5 MIM	6 DIM	7 NIM	8 SNIM	9 VMIM	- Clean
TRADES [44]	46.5	49.6	48.8	46.2	48.0	47.7	46.7	48.2	45.5	49.5	76.2
GAIRAT [45]	59.8	58.4	59.4	59.2	58.8	58.9	58.9	59.7	60.2	59.8	74.1
RPF [2]	56.4	51.3	55.8	56.6	54.4	52.6	53.9	53.3	49.9	50.1	69.4
DMAT [39]	64.3	66.2	66.4	65.9	65.4	64.4	64.1	65.8	65.1	65.6	75.9
ADP [41]	77.2	71.8	73.7	71.8	75.6	75.9	76.2	76.0	76.9	72.3	74.1
DiffPure [27]	53.2	52.4	53.7	55.8	53.9	53.4	52.6	54.7	53.0	52.3	73.6
<b>CAD(ours)</b>	<b>83.7</b>	<b>82.0</b>	<b>76.2</b>	<b>82.5</b>	<b>83.5</b>	<b>82.0</b>	<b>81.9</b>	<b>82.2</b>	<b>83.4</b>	<b>81.9</b>	<b>88.1</b>
<b>CAD<sup>†</sup>(ours)</b>	<b>83.5</b>	<b>84.0</b>	<b>84.1</b>	<b>82.6</b>	<b>84.3</b>	<b>83.8</b>	<b>84.2</b>	<b>82.2</b>	<b>83.9</b>	<b>81.4</b>	<b>87.8</b>

Table 2. Classification accuracy (%) on ImageNet-100.

Stage Attack	0 PGD	1 VNIM	2 FGSM	3 BIM	- Clean
w/o $L_{\text{virtual}}$	95.6	86.6	70.6	78.5	95.8
w/o $L_{\text{proto}}$	95.7	93.7	81.6	88.2	95.8
w/o $f_p$	95.8	93.4	83.8	94.7	55.9
<b>CAD(ours)</b>	<b>95.8</b>	<b>93.4</b>	<b>83.8</b>	<b>94.7</b>	<b>95.8</b>

Table 3. Classification accuracy (%) on CIFAR-10 for ablation.

Stage	0	1	2	3
number = 1	95.8	93.4	83.8	94.7
number = 2	95.8	88.5	93.5	92.8
number = 3	95.8	89.5	93.6	92.5

Table 4. Classification accuracy (%) on CIFAR-10 for different number of attacks in one stage.

ability in such scenarios, we evaluate the classification accuracy when faced with 1, 2, and 3 concurrent attacks. As presented in Tab. 4, when the number of attack increase to 2 and 3, the classification accuracy against these attacks still remain at a high level: 92.8% and 92.5% at stage 3 respectively. The results presented in Tab. 4 indicate that CAD continues to perform effectively even when confronted with multiple simultaneous attacks.

#### 5.4. Number of Shots for Adaptation

As indicated in Principle 2, the defense adaptation relies on few-shot defense feedback. To investigate the influence of the amount of feedback  $K$  per class, we conducted tests with  $K = 15, 10, 5, 1$ . The results presented in Tab. 5 illus-

Stage Attack	0 PGD	1 VNIM	2 FGSM	3 BIM
$K = 15$	95.8	93.7	81.2	94.8
$K = 10$	95.8	93.4	83.8	94.6
$K = 5$	95.8	93.2	80.8	93.7
$K = 1$	95.8	92.8	77.5	90.2

Table 5. Classification accuracy (%) on CIFAR-10 with different feedback scale  $K$ .

trate that defense performance diminishes as  $K$  decreases. Nevertheless, even with reduced  $K$ , CAD continues to efficiently defend against adversarial attacks (90.2% when  $K = 1$  at stage 3), highlighting its strong capability in few-shot scenarios.

#### 5.5. Memory Allowance for Adaptation

As outlined in Principle 3, we need to employ memory efficiently for continual defense. In order to demonstrate CAD's effectiveness in conserving memory, we conducted tests to measure the occupied memory space and model size at each stage. As depicted in Tab. 6, CAD requires neither a large cache footprint (with only a 25KB growth per stage) nor an expansion of the model size. This underscores our approach's ability to utilize efficient memory.

#### 6. Conclusion

The operational environment for defense systems is inherently dynamic, and it is unrealistic to expect a defense

Stage	Cache Size			Model Size		
	1	2	3	1	2	3
<b>CAD</b>	50.3K	75.5K	100.4K	141M	141M	141M
<b>CAD<sup>†</sup></b>	257M	377M	504M	280M	419M	558M

Table 6. Comparison of the Cache Size and Model Size (Byte) between CAD and premium-CAD on CIFAR-10.

method to address all types of attacks. As a response to this situation, we propose the first continual adversarial defense (CAD) framework, designed to dynamically adapt to a wide array of attacks as they emerge in sequential stages. In consideration of practical applicability, we have formulated four principles including few-shot feedback and memory-efficient adaptation, and CAD demonstrates strong performance when operating under these principles. Through experiments conducted on CIFAR-10 and ImageNet-100, we have demonstrated the effectiveness of our approach in combating multiple stages of various adversarial attacks, achieving significant improvements over baseline methods.

## 7. Acknowledgements

This work was supported in part by the Natural Science Foundation of China under Grant 61972169,62372203 and 62302186, in part by the National key research and development program of China(2022YFB2601802), in part by the Major Scientific and Technological Project of Hubei Province (2022BAA046, 2022BAA042), in part by the Knowledge Innovation Program of Wuhan-Basic Research, in part by China Postdoctoral Science Foundation 2022M711251.

## References

[1] Jia Deng, Wei Dong, Richard Socher, Li-Jia Li, Kai Li, and Li Fei-Fei. Imagenet: A large-scale hierarchical image database. In *CVPR*, 2009. 6

[2] Minjing Dong and Chang Xu. Adversarial robustness via random projection filters. In *CVPR*, pages 4077–4086, 2023. 7, 8

[3] Yinpeng Dong, Fangzhou Liao, Tianyu Pang, Hang Su, Jun Zhu, Xiaolin Hu, and Jianguo Li. Boosting adversarial attacks with momentum. In *CVPR*, pages 9185–9193, 2018. 6

[4] Yinpeng Dong, Tianyu Pang, Hang Su, and Jun Zhu. Evading defenses to transferable adversarial examples by translation-invariant attacks. In *CVPR*, pages 4307–4316, 2019. 3

[5] Spyros Gidaris and Nikos Komodakis. Dynamic few-shot visual learning without forgetting. In *CVPR*, pages 4367–4375, 2018. 6

[6] Ian J. Goodfellow, Jonathon Shlens, and Christian Szegedy. Explaining and harnessing adversarial examples, 2014. 3, 6

[7] Will Grathwohl, Kuan-Chieh Wang, Jörn-Henrik Jacobsen, David Duvenaud, Mohammad Norouzi, and Kevin Swersky. Your classifier is secretly an energy based model and you should treat it like one. In *ICLR*, 2020. 3, 6, 7, 8

[8] Kaiming He, Xiangyu Zhang, Shaoqing Ren, and Jian Sun. Deep residual learning for image recognition. In *CVPR*, pages 770–778, 2016. 6

[9] Mitch Hill, Jonathan Craig Mitchell, and Song-Chun Zhu. Stochastic security: Adversarial defense using long-run dynamics of energy-based models. In *ICLR*, 2020. 3, 8

[10] Hao Huang, Yongtao Wang, Zhaoyu Chen, Yuze Zhang, Yuheng Li, Zhi Tang, Wei Chu, Jingdong Chen, Weisi Lin, and Kai-Kuang Ma. Cmua-watermark: A cross-model universal adversarial watermark for combating deepfakes. In *AAAI*, pages 989–997, 2022. 2

[11] Yulun Jiang, Chen Liu, Zhichao Huang, Mathieu Salzmann, and Sabine Susstrunk. Towards stable and efficient adversarial training against  $l_1$  bounded adversarial attacks. In *ICML*, pages 15089–15104. PMLR, 2023. 7, 8

[12] Hoki Kim. Torchattacks: A pytorch repository for adversarial attacks. *arXiv preprint arXiv:2010.01950*, 2020. 6

[13] Alex Krizhevsky, Geoffrey Hinton, et al. Learning multiple layers of features from tiny images. *Technical report*, 2009. 6

[14] Alexey Kurakin, Ian Goodfellow, and Samy Bengio. Adversarial machine learning at scale, 2016. 3, 6

[15] Cassidy Laidlaw, Sahil Singla, and Soheil Feizi. Perceptual adversarial robustness: Defense against unseen threat models. In *ICLR*, 2020. 6, 8

[16] Yingwei Li, Song Bai, Yuyin Zhou, Cihang Xie, Zhishuai Zhang, and Alan Yuille. Learning transferable adversarial examples via ghost networks. In *AAAI*, pages 11458–11465, 2020. 2

[17] Jiadong Lin, Chuanbiao Song, Kun He, Liwei Wang, and John E Hopcroft. Nesterov accelerated gradient and scale invariance for adversarial attacks. In *ICLR*, 2019. 3, 6

[18] Yaoyao Liu, Yuting Su, An-An Liu, Bernt Schiele, and Qianru Sun. Mnemonics training: Multi-class incremental learning without forgetting. In *CVPR*, pages 12245–12254, 2020. 3

[19] Yaoyao Liu, Bernt Schiele, and Qianru Sun. Adaptive aggregation networks for class-incremental learning. In *CVPR*, pages 2544–2553, 2021.

[20] Yaoyao Liu, Bernt Schiele, and Qianru Sun. Rmm: Reinforced memory management for class-incremental learning. *NeurIPS*, 34:3478–3490, 2021.

[21] Yaoyao Liu, Yingying Li, Bernt Schiele, and Qianru Sun. Online hyperparameter optimization for class-incremental learning. In *AAAI*, 2022. 4

[22] Yaoyao Liu, Yingying Li, Bernt Schiele, and Qianru Sun. Online hyperparameter optimization for class-incremental learning. In *AAAI*, pages 8906–8913, 2023.

[23] Yaoyao Liu, Yingying Li, Bernt Schiele, and Qianru Sun. Wakening past concepts without past data: Class-incremental learning from online placebos. In *WACV*, 2023.

[24] Yaoyao Liu, Bernt Schiele, Andrea Vedaldi, and Christian Rupprecht. Continual detection transformer for incremental object detection. In *CVPR*, pages 23799–23808, 2023.

[25] Zilin Luo, Yaoyao Liu, Bernt Schiele, and Qianru Sun. Class-incremental exemplar compression for class-incremental learning. In *CVPR*, pages 11371–11380, 2023. 3

[26] Aleksander Madry, Aleksandar Makelov, Ludwig Schmidt, Dimitris Tsipras, and Adrian Vladu. Towards deep learning models resistant to adversarial attacks, 2017. 3, 6

[27] Weili Nie, Brandon Guo, Yujia Huang, Chaowei Xiao, Arash Vahdat, and Anima Anandkumar. Diffusion models for adversarial purification. In *ICML*, 2022. 3, 8

[28] Sylvestre-Alvise Rebiffé, Alexander Kolesnikov, Georg Sperl, and Christoph H Lampert. icarl: Incremental classifier and representation learning. In *CVPR*, pages 2001–2010, 2017. 3, 4, 5, 6

[29] Hadi Salman, Mingjie Sun, Greg Yang, Ashish Kapoor, and J Zico Kolter. Denoised smoothing: A provable defense for pretrained classifiers. *NeurIPS*, 33:21945–21957, 2020. 3

[30] Yuxuan Shi, Hefei Ling, Lei Wu, Jialie Shen, and Ping Li. Learning refined attribute-aligned network with attribute selection for person re-identification. *Neurocomputing*, 402: 124–133, 2020. 1

[31] Jake Snell, Kevin Swersky, and Richard Zemel. Prototypical networks for few-shot learning. *NeurIPS*, 30, 2017. 4, 6

[32] Olga Taran, Shideh Rezaifar, Taras Holotyak, and Slava Voloshynovskiy. Defending against adversarial attacks by randomized diversification. In *CVPR*, pages 11226–11233, 2019. 2, 3

[33] Yonglong Tian, Dilip Krishnan, and Phillip Isola. Contrastive multiview coding. In *Computer Vision–ECCV 2020: 16th European Conference, Glasgow, UK, August 23–28, 2020, Proceedings, Part XI 16*, pages 776–794. Springer, 2020. 6

[34] Florian Tramèr, Alexey Kurakin, Nicolas Papernot, Ian Goodfellow, Dan Boneh, and Patrick McDaniel. Ensemble adversarial training: Attacks and defenses. In *ICLR*, 2018. 6

[35] Florian Tramèr, Alexey Kurakin, Nicolas Papernot, Ian Goodfellow, Dan Boneh, and Patrick McDaniel. Ensemble adversarial training: Attacks and defenses. In *ICLR*, 2018. 6

[36] Vikas Verma, Alex Lamb, Christopher Beckham, Amir Najafi, Ioannis Mitliagkas, David Lopez-Paz, and Yoshua Bengio. Manifold mixup: Better representations by interpolating hidden states. In *ICML*, pages 6438–6447, 2019. 5

[37] Qian Wang, Yongqin Xian, Hefei Ling, Jinyuan Zhang, Xiaorui Lin, Ping Li, Jiazhong Chen, and Ning Yu. Detecting adversarial faces using only real face self-perturbations. In *IJCAI*, pages 1488–1496, 2023. Main Track. 6

[38] Xiaosen Wang and Kun He. Enhancing the transferability of adversarial attacks through variance tuning. In *CVPR*, pages 1924–1933, 2021. 3, 6

[39] Zekai Wang, Tianyu Pang, Chao Du, Min Lin, Weiwei Liu, and Shuicheng Yan. Better diffusion models further improve adversarial training. In *ICML*, 2023. 3, 7, 8

[40] Weibin Wu, Yuxin Su, Michael R. Lyu, and Irwin King. Improving the transferability of adversarial samples with adversarial transformations. In *CVPR*, pages 9020–9029, 2021. 3, 6

[41] Jongmin Yoon, Sung Ju Hwang, and Juho Lee. Adversarial purification with score-based generative models. In *ICML*, pages 12062–12072, 2021. 2, 3, 7, 8

[42] Sergey Zagoruyko and Nikos Komodakis. Wide residual networks. *arXiv preprint arXiv:1605.07146*, 2016. 6

[43] Chi Zhang, Nan Song, Guosheng Lin, Yun Zheng, Pan Pan, and Yinghui Xu. Few-shot incremental learning with continually evolved classifiers. In *CVPR*, pages 12455–12464, 2021. 3, 4

[44] Hongyang Zhang, Yaodong Yu, Jiantao Jiao, Eric Xing, Laurent El Ghaoui, and Michael Jordan. Theoretically principled trade-off between robustness and accuracy. In *ICML*, pages 7472–7482, 2019. 2, 3, 6, 7, 8

[45] Jingfeng Zhang, Jianing Zhu, Gang Niu, Bo Han, Masashi Sugiyama, and Mohan Kankanhalli. Geometry-aware instance-reweighted adversarial training. In *ICLR*, 2020. 3, 7, 8

[46] Yixiao Zhang, Xinyi Li, Huimiao Chen, Alan L. Yuille, Yaoyao Liu, and Zongwei Zhou. Continual learning for abdominal multi-organ and tumor segmentation. In *MICCAI*, pages 35–45. Springer, 2023. 3

[47] Zhilu Zhang and Mert Sabuncu. Generalized cross entropy loss for training deep neural networks with noisy labels. In *NeurIPS*, 2018. 5

[48] Da-Wei Zhou, Fu-Yun Wang, Han-Jia Ye, Liang Ma, Shiliang Pu, and De-Chuan Zhan. Forward compatible few-shot class-incremental learning. In *CVPR*, pages 9046–9056, 2022. 3, 5, 6

[49] Fei Zhu, Zhen Cheng, Xu-yao Zhang, and Cheng-lin Liu. Class-incremental learning via dual augmentation. In *NeurIPS*, pages 14306–14318, 2021. 3

[50] Fei Zhu, Xu-Yao Zhang, Chuang Wang, Fei Yin, and Cheng-Lin Liu. Prototype augmentation and self-supervision for incremental learning. In *CVPR*, pages 5871–5880, 2021. 5

[51] Kai Zhu, Wei Zhai, Yang Cao, Jiebo Luo, and Zheng-Jun Zha. Self-sustaining representation expansion for non-exemplar class-incremental learning. In *CVPR*, pages 9296–9305, 2022. 3, 5

# Continual Adversarial Defense

## Supplementary Material

### A. Weight Estimator Base on Self-Perturbation

In CAD, we use clean images  $\mathcal{D}_{\text{train}}$  and self-perturbation to train a weight estimator to ensemble the target model and the defense model. We craft half of the real images to pseudo adversarial images as negative samples and label other real images as positive samples. Then, we train a 4-layer ConvNet as the weight estimator  $f_p$  in a binary classification manner. In this section, we introduce the details of self-perturbation and model ensemble.

---

#### Algorithm 2 Self-perturbation

---

**Input:** A empty perturbation matrix  $\eta^p \in \mathbb{R}^{H \times W \times 3}$  with the same shape of real image  $\mathbf{x}^r$ .  
**Parameter:** Max perturbation magnitude  $\epsilon$ , pattern mode.  
**Output:** Self-perturbed image  $\mathbf{x}^p$ .

- 1: A random direction matrix  $R = \{\vec{r}_{ij}\} \in \mathbb{R}^{H \times W \times 3}$ .
- 2: **for**  $\vec{r}_{ij}$  **in**  $\eta^p$  **do**
- 3:   Select random noise value  $\alpha$ .
- 4:   **if** pattern mode **is** ‘point-wise’ **then**
- 5:      $\vec{\eta}_{ij} := \alpha \cdot \vec{r}_{ij}$ .
- 6:   **else if** pattern mode **is** ‘block-wise’ **then**
- 7:     Select a random neighborhood  $A_{ij}$  of  $\vec{r}_{ij}$ .
- 8:     **for**  $\vec{r}_{ijk}$  **in**  $A_{ij}$  **do**
- 9:        $\vec{\eta}_{ijk} := \alpha \cdot \vec{r}_{ij}$ .
- 10:     **end for**
- 11:   **end if**
- 12: **end for**
- 13: Clip perturbation  $\eta^p$  using Equation 11.
- 14: Generate self-perturbed image  $\mathbf{x}^p$  using Equation 12.
- 15: **return**  $\mathbf{x}^p$

---

**Self-Perturbation** As presented in Algorithm 2, we perturb each point in the point-wise pattern and each block in the block-wise pattern in a stochastic direction, where blocks are random neighborhoods of a set of scattered points. The generated perturbation image  $\eta^p$  is constrained in  $l^\infty$  norm, and clipped according to  $\epsilon$ ,

$$\eta^p = \text{Clip}_{[-\epsilon, \epsilon]}(\eta^p). \quad (11)$$

A self-perturbed image is calculated as

$$\mathbf{x}^p = \mathbf{x}^r + \eta^p. \quad (12)$$

**Model Ensemble** Trained with self-perturbation, the weight estimator  $f_p$  is able to distinguish between the clean

and adversarial images. The output logit  $\mathbf{w}$  of  $f_p$  represents the probability of an image to be clean or adversarial. Therefore, we use  $\mathbf{w}$  to ensemble the target model and the defense model:

$$\text{logit}_i(\mathbf{x}) = \mathbf{w} \cdot [f_t(\mathbf{x}), f_i(\mathbf{x})]^\top \quad (13)$$

In this way, both the clean images and the adversarial images are correctly classified.

### B. Premium-CAD

We propose another variant of our method denoted as premium-CAD in the case of no constraint of memory and no concerns about the amount of feedback. In each stage, we train an attack-specific defense model using abundant feedback and ensemble the target model and all the defense models by a stage-evolved weight estimator.

**Attack-Specific Defense Model** In stage 0, the initial defense model is optimized under the full supervision using adversarial dataset  $\mathcal{A}_{\text{train}}^0 = \{(\mathbf{x}_{\text{adv}}^0, y) | \mathbf{x}_{\text{adv}}^0 = A_0(\mathbf{x}), (\mathbf{x}, y) \in \mathcal{D}_{\text{train}}\}$ . In stage  $i$ , another defense model is trained using abundant feedback  $\mathcal{A}_{\text{train}}^i = \{(\mathbf{x}_{\text{adv}}^i, y)\}_{N \times K}$  where  $N$  is the number of classes in dataset  $\mathcal{D}_{\text{train}}$  and  $K$  is the amount of feedback per class. The scale of feedback is set to  $K = 10$  in CAD and  $K = 1000$  in premium-CAD.

In this way, we have  $i + 1$  defense models in stage  $i$ . The defense model is designed to tackle adversarial examples from a specific attack, complementing each other.

---

#### Algorithm 3 Premium Continual Adversarial Defense

---

**Input:** Benign dataset  $\mathcal{D}_{\text{train}}$ , abundant feedback  $\mathcal{A}_{\text{train}}^i$  generated by attack  $A_i$  for stage  $i = 1, \dots, T$ .

**Output:** Defense model ensemble.

- 1: **for**  $i$  **in**  $1, \dots, T$  **do**
- 2:   Train an attack-specific defense model  $f_i$ .
- 3:   Train a stage-evolved weight estimator  $f_p^i$ .
- 4:   Ensemble the defense models  $[f_0, f_1, \dots, f_i]$  and the target model  $f_t$  using Eq. (13).
- 5: **end for**

---

**Stage-Evolved Weight Estimator** To ensemble the target model  $f_t$  and defense models  $[f_0, f_1, \dots, f_i]$ , we use a joint dataset  $\mathcal{D}_J^i = \bigcup_{i=0,1,\dots,i} \mathcal{A}_{\text{train}}^i \cup \mathcal{D}_{\text{train}}$  to train the weight estimator  $f_p^i$  in stage  $i$ . Feed an image to the weight estimator  $f_p^i$ , it output a weight vector  $\mathbf{w}^i \in \mathbb{R}^{i+2}$  to ensemble

models:

$$\mathbf{w}^i = f_i(\mathbf{x}) \quad (14)$$

The final output for premium-CAD is:

$$\text{logit}_i(\mathbf{x}) = \mathbf{w}^i \cdot [f_t(\mathbf{x}), f_0(\mathbf{x}), f_1(\mathbf{x}), \dots, f_i(\mathbf{x})]^\top \quad (15)$$

The overall algorithm of premium-CAD framework is presented in Algorithm 3. The loss function for training attack-specific defense models and stage-evolved weight estimators is Cross-Entropy Loss.